TITLE: Adaptive resistance to FLT3 inhibitors is potentiated by ROS-driven DNA repair signalling

AUTHORS: Dilana E. Staudt[1,*], Zacary P. Germon[1,2,3,*,†], Abdul Mannan[1,2,*], Tabitha McLachlan[1,2,*], Heather C. Murray[2,4], Ryan J. Duchatel[1,2,3], Bryce C. Thomas[1,2,3], Tyrone Beitaki[1,2,3], Holly P. McEwen[1,2,3], Mika L. Persson[1,2,3], Leah Calvert[5,6], Izac J. Findlay[1,2,3], , Evangeline R. Jackson[1,2,3], Nathan D. Smith[7], David A. Skerrett-Byrne[5,6,8,9] , David Mossman[10], Brett Nixon[5,6], Geoffry De Iullis[5,6], Alicia M. Douglas[1], Anoop K. Enjeti[2,10,11], Jonathan R. Sillar[1,2,10], Janis Chamberlain[1,12], Frank Alvaro[2,12], Andrew H. Wei[13], Patrick Connerty[14], Nicole Verrills[2,4], Matthew D. Dun[1,2,3,†]

CONTRIBUTIONS: * These authors contributed equally as co-first authors of this study.

AFFILIATIONS:

[1] Cancer Signalling Research Group, School of Biomedical Sciences and Pharmacy, College of Health, Medicine and Wellbeing, University of Newcastle, Callaghan, NSW, Australia

[2] Precision Medicine Research Program, Hunter Medical Research Institute, New Lambton Heights, NSW, Australia; and School of Biomedical Sciences and Pharmacy, College of Health, Medicine and Wellbeing, University of Newcastle, Callaghan, NSW, Australia

[3] Paediatric Stream, Mark Hughes Foundation Centre for Brain Cancer Research, College of Health, Medicine, and Wellbeing, Callaghan, NSW, Australia

[4] Molecular Oncology Group, School of Biomedical Sciences and Pharmacy, College of Health, Medicine and Wellbeing, University of Newcastle, Callaghan, NSW, Australia

[5]School of Environmental and Life Sciences, College of Engineering, Science and Environment, University of Newcastle, Callaghan, NSW, Australia.

[6] Infertility and Reproduction Research Program, Hunter Medical Research Institute, New Lambton Heights, NSW, Australia.

[7] Analytical and Biomolecular Research Facility (ABRF), Research Services, University of Newcastle, Callaghan, NSW, Australia.

[8] Institute of Experimental Genetics, Helmholtz Zentrum München, German Research Center for Environmental Health Neuherberg, Germany.

[9] German Center for Diabetes Research (DZD) Neuherberg, Germany

[10] Division of Molecular Medicine, Pathology North John Hunter Hospital, New Lambton Heights, NSW, Australia.

[11] Calvary Mater Hospital, Haematology Department, Waratah, NSW Australia.

[12] John Hunter Children's Hospital, School of Medicine and Public Health, College of Health, Medicine and Wellbeing, University of Newcastle, New Lambton Heights, NSW Australia.

[13] Department of Clinical Haematology, The Alfred Hospital and Monash University, Melbourne, VIC, Australia.

[14] Children's Cancer Institute, Lowy Cancer Research Centre, School of Clinical Medicine, UNSW Medicine & Health, UNSW Centre for Childhood Cancer Research, UNSW Sydney, Sydney, NSW, Australia

* These authors contributed equally as co-first authors of this study.

RUNNING TITLE: Targeting ATM as a salvage therapy for paediatric and adult AML

† **CORRESPONDING AUTHORS:** Matthew D. Dun – Matt.Dun@newcastle.edu.au and Zacary P. Germon – Zacary.Germon@newcastle.edu.au

DATA SHARING STATEMENT: The mass spectrometry proteomics data has been deposited to the ProteomeXchange Consortium (http://proteomecentral.proteomexchange.org) via the PRIDE partner repository with the dataset identifier PXD053329 and 10.6019/PXD053329

CONFLICT OF INTEREST: The authors declare no potential conflicts of interest.

MANUSCRIPT FEATURES: Manuscript - Abstract: 250 words, main text: 4020 words, 6 Figures. Supplementary Information - Supplementary Materials and Methods, 4 Supplementary Figures. Supplementary Excel file - 11 Supplementary Tables.

ABSTRACT

Alterations in the FMS-like tyrosine kinase 3 (FLT3) gene are the most frequent driver mutations in acute myeloid leukaemia (AML), linked to a high risk of relapse in patients with internal tandem duplications (FLT3-ITD). Tyrosine kinase inhibitors (TKIs) targeting the FLT3 protein are approved for clinical use, yet resistance often emerges. This resistance is mainly seen following the acquisition of additional point mutations in the tyrosine kinase domain (TKD), resulting in a double mutant FLT3-ITD/TKD, which sustains cell signalling and survival despite the presence of FLT3 inhibitors. Here, we developed a FLT3-mutant AML model with adaptive resistance to type II TKIs, sorafenib, and quizartinib by *in vitro* drug selection. Through global multiomic profiling, we identified upregulation of proteins involved in reactive oxygen species (ROS) production, particularly NADPH-oxidases, driving cellular 'ROS-addiction', with resistant cells relying on ROS for survival, and genome fidelity preserved by ATM-driven DNA repair. Transcriptomic analysis of adult and paediatric AML (pAML) patients identified high ATM expression as a biomarker for shorter median overall survival in both the de novo and relapsed settings. Inhibition of ATM with clinically relevant therapy WSD-0628 effectively killed TKI- and chemotherapy-resistant AML cells *in vitro* and significantly extended the survival of mice with sorafenib- and quizartinib-resistant FLT3-ITD AML *in vivo*. We propose a new treatment strategy to improve survival of patients who develop resistance to sorafenib and quizartinib, as well as relapsed and refractory pAML, exploiting resistance mechanisms to precision therapies and cell-intrinsic features of high-risk cases, highlighting a clinically relevant salvage strategy.

KEYWORDS: acute myeloid leukaemia (AML); paediatric AML (pAML); tyrosine kinase inhibitors; FLT3; resistance; relapsed refractory; DNA damage; DNA repair; ATM signalling; sorafenib; quizartinib; WSD-0628; reactive oxygen species; ROS; salvage strategy

Word count: 250

INTRODUCTION

Constitutive activation of the FMS-like Tyrosine Kinase 3 receptor (FLT3; CD135) following the acquisition of genetic mutations is seen in 20-30% of acute myeloid leukaemia (AML) cases (1), leading to high relapse risk and poor survival (2, 3). FLT3, a type III receptor tyrosine kinase (RTK-III), regulates haematopoietic cell differentiation, proliferation, and survival (4). Binding of FLT3 ligand (FLT3L) activates ERK/MAPK (5), JAK/STAT (6), and PI3K/AKT signalling (7). The most common FLT3 mutations in AML are internal tandem duplications (FLT3-ITD; 20-25%) (8), followed by point mutations in the second tyrosine kinase domain (FLT3-TKD; 5-10%) (8, 9) both causing constitutive FLT3 activation and oncogenic signalling (9).

The high prevalence of FLT3 mutations in AML has led to the development and clinical assessment of first- and second-generation tyrosine kinase inhibitors (TKIs) (1, 10, 11). However, single-agent TKI therapies often fail long-term due to unsustained anti-leukaemic responses and secondary resistance (10-12). Midostaurin (PKC412) was the first TKI approved for newly diagnosed FLT3-mutant AML with standard cytarabine and anthracycline therapy in 2017 (13). Quizartinib (AC220), a second-generation FLT3 inhibitor, was approved in 2023 for use with standard therapy and as maintenance monotherapy (14). Gilteritinib is approved for relapsed/refractory AML (R/R-AML) with FLT3 mutation (15). Several other TKIs are in clinical assessment for AML (Supplementary Table S1).

Sorafenib, initially approved for solid tumours, shows promise in FLT3-ITD AML as a maintenance therapy post-allo-HCT, improving relapse-free survival and as salvage therapy for post-allo-HCT relapses (16). It is extensively studied for FLT3-mutant paediatric AML (pAML) (17), offering multi-kinase inhibition, including FLT3, to combat resistance and improve outcomes.

Despite initial improvements, resistance to FLT3-targeted therapies persists (10-12), caused by FLT3L overexpression (18), clonal selection (19), bone marrow stromal protection (20), off-target mutations, FLT3-independent/ downstream signalling pathway activation (21),

or through additional mutations in FLT3 (FLT3-ITD/TKD) affecting drug binding sites (1, 10, 22, 23). Mutations at residues D835 (10, 12, 24), Y842 (22, 23), F691 (23), N676 (22), and A627 (23) confer resistance to type I and/or II TKIs.

Understanding oncogenic signalling pathways active in high-risk and resistance settings aids precision medicine. This study integrates next-generation sequencing (NGS), phosphoproteomics, and patient transcriptomics to identify upregulation of the oxidative stress-driven ATM DNA repair signalling pathway in therapy-resistant AML, effectively targeted by the novel ATM inhibitor, WSD-0628. These findings support early-phase trials for R/R AML or high-risk pAML.

MATERIALS AND METHODS

Detailed materials and methods can be found in the Supplemental Information.

Study approval.

The use of patient-derived human AML cell lines was approved by the Human Ethics Research Committee, University of Newcastle (H-2018-0241). All *in vivo* studies were approved by the University of Newcastle Animal Care and Ethics Committee (A-2017-733, A-2023-308).

In vitro development of adaptive resistance

TKI and standard-of-care resistant MV4-11 cells were developed through serial passaging of cells in increasing doses of sorafenib (Selleckchem, Houston, TX, USA) from 2.5 nM-1280 nM over 20 weeks or cytarabine (Selleckchem) from 10 μM-500 μM followed by daunorubicin (Sigma-Aldrich, Burlington, MA, USA) from 2 nM-12 nM. Cells were DNA sequenced by next generation sequencing (Supplementary Table S2) using the Myeloid Solution panel, as described in Supplemental Information.

Structural modelling of tyrosine kinase inhibitors binding to FLT3

Several crystal structures detailing the intracellular domains of FLT3, including the inactive conformation of the TKDs were used as templates to create a multiple sequence alignment homology model of the inactive kinase as previously described (25).

pHASED phosphoproteomics

Quantitative phosphoproteomics of MV4-11 parental and TKI resistant cells was performed as previously described (26). The mass spectrometry proteomics data is deposited to the ProteomeXchange Consortium via the PRIDE partner repository (27) with the dataset identifier PXD053329 and 10.6019/PXD053329. Reviewer access via the PRIDE website - **Username:** reviewer_pxd053329@ebi.ac.uk **Password:** lTeh0PPlMcFj

Analysis of publicly available patient survival and expression data

RNA-seq and clinical data from the Therapeutically Applicable Research to Generate Effective Treatments (TARGET) and Beat AML initiatives was minded and analysed using GraphPad Prism Software (version 10.0.2, GraphPad, Boston, MA, USA) (28).

Detection of reactive oxygen species

Dihydroethidium (DHE) (Life Technologies, Australia) was used to detect intracellular cytoplasmic superoxide as previously described (29).

ATM knockdown

MV4-11 sensitive and resistant cell lines were transfected using RNAiMAX lipofectamine reagent (Invitrogen, Carlsbad, CA) as per manufacturer's instructions with ATM–specific small interfering RNA (siRNA) or a scrambled siRNA control.

Terminal Deoxynucleotidyl Transferase dUTP Nick End Labelling (TUNEL) DNA Fragmentation Assay and Oxidative DNA Damage Assessment by 8-hydroxy-2'-deoxyguanosine (8-OHdG)

MV4-11 FLT3-ITD sensitive and TKI resistant cell lines were treated with either 250 nM WSD-0628 for 24 h, 1 mM H_2O_2 for 30 min or ATM-siRNA or scramble control and assessed for formation of TUNEL or oxidative DNA damage through 8-OHdG ICC fluorescence (30).

AML xenograft mouse modelling

NOD-*Rag1*^{null} *IL2rg*^{null} (NRG) mice were engrafted with FLT3-ITD TKI sensitive or resistant, MV4-11-luc cells (1e^6 cells in PBS) by tail vein injection. Bioluminescence imaging (BLI) was used to detect leukemic cell engraftment, and randomized for treatment once BLI reached a mean radiance of 1 × 10^6 p/s. Mice were treated with either vehicle control, sorafenib (10 mg/kg/day MV4-11 resistant; 2.5 mg/kg/day MV4-11 sensitive), quizartinib (2 mg/kg/day) or WSD-0628 (5 mg/kg/day) as monotherapies, or in combination, for four weeks. Mice were euthanized at ethical endpoint, including weight loss exceeding 20% or body condition scores indicating ethical endpoint.

RESULTS

Establishment of a human cell line model of adaptive TKI resistance

Dual FLT3-ITD and D835V/Y mutations are a known mechanism of resistance to type II TKIs. Previously, we generated isogenic FLT3-ITD AML cell line models with these mutations (24). Quantitative proteomics identified the activation of the ATM pathway, promoting cell survival despite high dose sorafenib (26). Here, we have expanded these studies by developing a human FLT3-ITD AML cell line (MV4-11) model of adaptive resistance to type II TKIs by treating cells with increasing sorafenib doses (0 nM - 1280 nM) (Supplementary Figure S1). Next generation sequencing (NGS) was performed on the sorafenib resistant cell line, identifying the acquisition of a point mutation in residue 842 in the second TKD (TKD2), resulting in the substitution of tyrosine (Y) for cysteine (C), thus generating a double mutant FLT3-ITD/Y842C receptor (Supplementary Table S2).

Treatment of these cells with type II TKIs sorafenib (Figure 1A) and quizartinib (Figure 1B), resistant cells showed an 80-fold (p=0.0003; area under the curve (AUC) 2-fold, p≤0.0001), and 881.5-fold (p=0.004; AUC 3.7-fold, p≤0.0001) increase in IC_{50} compared to FLT3-ITD sensitive cell lines, respectively (Supplementary Table S3). Consistent with previous reports of TKD2 mutations (22), these TKI resistant cells (FLT3-ITD/Y842C) showed increased sensitivity to type I TKIs midostaurin (IC_{50} 0.50-fold, p=0.01; AUC 0.73-fold, p=0.01) (Figure 1C), and crenolanib (IC_{50} 0.90-fold, p=0.04; AUC 0.85-fold, p=0.02) (Figure 1D) compared to the sensitive cells (Supplementary Table S3). No increase in Annexin V/PI staining was seen in TKI resistant cells treated with either sorafenib (mean viability = 88.2%) or quizartinib (mean viability = 85.9%). In contrast, treatment with the type II TKIs midostaurin (mean viability = 69.4%, $p \leq 0.0001$) or crenolanib (mean viability = 38.2%, $p \leq 0.0001$) promoted cell death. This effect was particularly notable in resistant cells compared to FLT3-ITD sensitive cell lines ($p \leq 0.0001$) (Figure 1E-F; Supplementary Table S4).

Acquisition of FLT3-TKD2 mutations impact sorafenib and quizartinib binding

FLT3 is a 993 amino acid receptor tyrosine kinase with five immunoglobulin-like extracellular domains, a transmembrane domain, a cytoplasmic juxtamembrane (JM) domain, and two intracellular tyrosine kinase domains (TKD) (Figure 2A) (4). FLT3-ITD mutations disrupt the JM domain's auto-inhibitory function, switching the receptor to its active conformation without FLT3L binding (31). To understand type II TKI resistance due to TKD2 point mutations, we performed *in silico* mutagenesis of the FLT3-TKD activation loop (aa 829 - aa 858) and analysed sorafenib and quizartinib binding (Figure 2B-E). Our resistance model includes ITD and a Y842C mutation in the second TKD (Supplementary Table S2). Both D835 and Y842 are within the activation loop and are inaccessible during auto-inhibitory conformation (Figure 2B-D) (9, 32). Type II TKIs (sorafenib and quizartinib) bind to the ATP-binding pocket of inactive FLT3 (yellow) (Figure 2B), while the active conformation sterically blocks binding due to phenylalanine 855 (F855) in the ‘back pocket’ (Figure 2D).

Studies show that D835 and Y842 mutations cause loss of key hydrophobic and hydrogen bond interactions, destabilising the auto-inhibitory conformation and promoting the active loop, reducing drug affinity, especially with ITD mutations (9). ChemPLP binding affinity scores from *in silico* modelling (25) indicated reduced binding efficiency for quizartinib and sorafenib with TKD mutations. For FLT3-ITD/TKD-Y842C resistant cells, quizartinib binding decreased from 83.28 (ITD alone) to 78.17 (with Y842C), and sorafenib binding from 62.52 to 57.51 (Figure 2E). Thus, TKD point mutations decrease drug binding affinity by altering the activation loop conformation (Figure 2C-D).

TKI resistant cells carry an increased dependency on DNA damage and repair pathways for survival

Differential signalling pathway analysis in resistance to type II TKIs, we performed by global, quantitative phosphoproteomics (n=3 independent biological replicates per cell line). Here we identified 1,469 unique phosphoproteins and 6,645 unique phosphorylated peptides (FDR 1%), with 1,335 phosphopeptides (20.1%) shown to be significantly altered in resistant cells to sensitive ($p \leq 0.05$). Two major clusters were shown to be differentially regulated in resistance ($\log_2 \pm 0.5$, $p \leq 0.05$) (Figure 3A; Supplementary Table S5). Alterations in cell death and survival ($p \leq 0.01$), and DNA replication, recombination and repair ($p \leq 0.009$) were identified amongst the molecular and cellular functions modified by differential phosphorylation in both clusters (Figure 3B*;* Supplementary Table S6).

Indeed, constitutive DNA damage and repair (DDR) has previously been found to contribute to disease progression and therapeutic response in haematological malignancies, including FLT3-mutant AML (33). Analysis of the phosphorylation changes in resistant vs sensitive cells in DDR proteins identified BRCA1 (log_{10} p=6.82), ATM (log_{10} p=6.57), and Nucleotide excision repair (NER) (log_{10} p=6.26) pathways as the top 3 DDR-associated signalling pathways in resistance (Figure 3C; Supplementary Table S7) corroborating studies

of resistance signalling in FLT3-ITD/D835V/Y mutations (26). Accordingly, Kinase-Substrate Enrichment Analysis (KSEA) predicted the key DDR kinases, DNA-dependent Protein Kinase PRKDC (DNA-PK; *z-score* = 1.99, *p*=0.02), and ATM kinase (*z-score*= 1.01), to be increased in activity in TKI resistant cells with a positive *z-score* indicating activation (Figure 3D*;* Supplementary Table S8). Protein-protein interaction analysis of DDR kinases identified by KSEA with a positive z-score (indicating activation) revealed four separate nodes of kinase interaction, predominantly connected through the ATM kinase (Figure 3E), validated by immunoblotting (Figure 3F). Increase in phosphorylation of the key DNA damage marker H2AX (S139) was seen in resistant cells (*p*=0.006) (Figures 3F-G), so we analysed the phosphoprotein changes in key proteins regulating ATM-driven DDR signalling (log_2 ± 0.5) (Figure 3H, Supplementary Table S9), including the Double-Strand Break (DSB) repair protein MRE11 (S688; S689; *p*=0.03), whereas its DNA repair inhibitory site (S649) was significantly decreased in phosphorylation (*p*=0.01). Increased phosphorylation of the activating sites of DNA-PK, S2612 (log_2 fold=2.4) and S2609 (log_2 fold=1.3), as well as cellular tumour antigen p53, S392 (log_2 fold=0.5), were also identified via phosphoproteomics (Figure 3H) and confirmed via immunoblotting (Figure 3F).

TKI resistant cells show decreased cell growth and proliferation

Alterations in cell cycle regulation were significantly overrepresented in the cluster with decreased phosphorylation in resistant cells (Figure 3B; Supplementary Table S6). IPA analysis predicted significant associations between phosphorylation changes in TKI-resistant cells and G2/M (log10 p=4.58) and G1/S (log10 p=3.29) cell cycle checkpoint regulation (Figure 3C; Supplementary Table S7). Given that cell cycle checkpoint activation controls DDR response (34), we assessed growth profiles of FLT3-ITD sensitive and resistant cell lines using cell proliferation (Figure 3I-J) and cell cycle (Figure 3K) assays.

Resistant cells displayed a 1.36-fold decrease in cell proliferation at the 48-hour timepoint compared to sensitive cells (p=0.02) (Figure 3I-J). Flow cytometry analysis showed differences in all cell cycle phases between sensitive and resistant lines, with a higher percentage of resistant cells in the S phase at 24 and 48 hours (p=0.01), and in the G2/M phase at 72 hours (p=0.03) (Figure 3K; Supplementary Table S10).

High ATM expression associated with worse overall outcomes in in paediatric AML and FLT3-mutant adult AML

To assess the clinical relevance of ATM expression in AML, we examined ATM expression in adult FLT3-ITD mutant patients at diagnosis and paediatric patients at diagnosis, progression, and relapse, using data from the Beat AML and Therapeutically Applicable Research to Generate Effective Treatments (TARGET) databases (33,34). In FLT3-ITD AML patients, high ATM expression is associated with shorter median overall survival (OS) compared to low ATM expression (n=68; *p*=0.019; 95% CI=1.1886 log-rank) (Figure 4A). Among paediatric patients, high ATM expression is linked to shorter event-free survival (n=239; *p*=0.012; 95% CI=1.1489 log-rank) (Figure 4B), shorter OS (*p*=0.013, 95% CI=1.565 log-rank) (Figure 4C), and shorter OS at relapse (n=125, *p*=0.048, 95% CI=1.552 log-rank) (Figure 4D). Increased ATM expression was observed at relapse compared to diagnosis (n=242, *p*=0.0015, Two-Tailed Welsch T-Test) (Figure 4E).

To evaluate the sensitivity of paediatric AML cells treated with the clinically relevant brain-penetrant ATM inhibitor WSD-0628, we exposed standard-of-care sensitive (SOC) sensitive and resistant AML cells (cytarabine and daunorubicin) for 48 h and measured viability. Both SOC sensitive and resistant cells demonstrated high sensitivity to WSD-0628, however, SOC-resistant cells were significantly more sensitive than SOC-sensitive cells (*p*≤0.0001, Two-Way ANOVA) (Figure 4F).

Type II TKI resistant cells reside in a state of high-level oxidative stress and oxidative DNA damage

Activation of DDR pathways, including ATM signalling, is triggered by the presence of DNA DSBs (35) commonly caused by excessive levels of ROS, considered a driver of disease progression in FLT3-mutant AML (29, 36, 37). Additionally, FLT3 inhibition itself is reported to result in the accumulation of ROS, consequently activating ATM signalling to maintain redox homeostasis (38). Commensurate with SOC resistant AML cells and patients (36, 37, 39), TKI-resistant cells showed increased cytoplasmic superoxide (DHE positive fluorescence) compared to sensitive cells, with a 1.93-fold increase in ROS levels (p=0.004) (Figure 5A-B). We next tested cell proliferation following treatment with the ROS scavenger N-Acetylcysteine (NAC, 1.25–20 mM). TKI-resistant cell lines showed significantly higher proliferation rates in 20 mM NAC (p=0.03) (Figure 5C). Phosphoproteomic analysis of ROS-associated canonical pathways in resistant cells identified significant increases in the ERK/MAPK (log10 p=8.9), PI3K/AKT (log10 p=3.5), and NRF2-mediated oxidative stress response (log10 p=1.45) pathways (Figure 5D).

Based on these data, we assessed whether the increased levels of ROS could result from differences in the expression of the NADPH oxidases (NOX2/4). Indeed, phosphoproteomic analysis identified ELF1 and IRF8 transcription factors as differentially phosphorylated in resistance, responsible for the transcriptional regulation of NOX2 and its associated subunits (Figure 5E) (40). Consistent with these findings, NOX2 and NOX4 protein expression showed increased expression in TKI resistant cells (Figure 5F). Finally, assessment of DNA damage in resistant cells revealed similar levels of DNA fragmentation in FLT3-ITD sensitive and TKI resistant cells under normal conditions. However, blocking DNA repair via inhibition of ATM using WSD-0628, resulted in a significant increase in DNA fragmentation in TKI resistant cells (3.8-fold, p=0.008) (Figure 5G). Similarly, blocking DNA repair through the pharmacological inhibition of ATM led to a significant increase in oxidative DNA damage in resistance, indicated by the presence of the oxidized DNA nucleoside

guanosine (8-OHdG) (Figure 5H). Equally, molecular inhibition of ATM (Figure 5I) led to a significant increase in oxidative DNA damage, analogous to that seen with WSD-0628 treatment, restricted to TKI resistant cells (Figure 5H).

ATM inhibition reduced cell proliferation in vitro and increased survival in vivo

To assess the therapeutic potential of targeting DDR signalling following the development of adaptive resistance to type II TKIs, we performed cytotoxicity analysis of FLT3-ITD sensitive and TKI resistant cells using the DNA-PK inhibitor peposertib (formerly known as M3814), ATM inhibitor KU-60019, and a second, more potent brain penetrant ATM inhibitor, WSD-0628, as single agents (Supplementary Figure S3A-C). Both FLT3-ITD sensitive and TKI resistant cell lines responded to DNA repair inhibition to all three single agents. Treatment with peposertib (Supplementary Figure S3A) and KU-60019 (Supplementary Figure S3B) did not show significant differences in sensitivity between FLT3-ITD sensitive and TKI resistant cells, even in the micromolar dose range. However, Both TKI sensitive and resistant cells showed nanomolar sensitivity to WSD-0628, with TKI resistant cells significantly more sensitive (IC_{50} 116.5 nM TKI resistant; IC_{50} 183.1 nM FLT3-ITD sensitive; AUC resistant vs sensitive 0.60-fold, p=0.003) (Figure 6A-C, Supplementary Figure S3C). We assessed the response of TKI resistant cells to WSD-0628 alone, and in combination with the type II TKIs sorafenib or quizartinib (Figure 6A-C, Supplementary Figure S3D, E). The combination of sorafenib with WSD-0628 (sorafenib 31.2 nM + WSD-0628 125 nM) significantly decreased cell proliferation by 1.8-fold (p=0.0008) compared to treatment with sorafenib alone (Figure 6A, Supplementary Figure S3D). A similar response was seen for quizartinib (quizartinib 12.5 nM + WSD-0628 125 nM), with a 1.6-fold reduction (p≤0.0001) (Figure 6B, Supplementary Figure S3E). Drug combinations were then assessed for synergistic interactions via the computational synergy analysis BLISS, however, both combinations only showed additive effects (Bliss score WSD-0628 + sorafenib: 4.09; Bliss score WSD-0628 + quizartinib: 4.68) (Supplementary Figure S3F, S3G, respectively) (41)

(Figure 6A-B). Consistently, treatment with WSD-0628 alone and in combination with sorafenib, or quizartinib, promoted significant levels of cell death compared to the untreated controls and either sorafenib or quizartinib alone (mean viability = 56.1%, p=0.0001 and 51.4%, p≤0.0001 respectively) (Figure 6C, Supplementary Table S11).

To evaluate the downstream signaling response to WSD-0628 alone or in combination, changes in ATM kinase and associated DNA damage and repair proteins were assessed via immunoblotting. ATM auto-phosphorylates at S1981 in response to DNA damage (35), and promotes chromosome relaxation by phosphorylating KAP1 at S824 (42). Phosphorylation induces KAP1 co-localisation with γH2AX at damage sites, facilitating homologous recombination (HR) and non-homologous end joining (NHEJ) repair (42, 43). Treatment with WSD-0628 alone or combined with TKIs decreased phosphorylation of ATM (S1981) and H2AX (S139) in TKI-resistant cells, while TKI treatment alone did not (Figure 6D).

To evaluate the anti-AML potential of ATM inhibition, we engrafted NOD-*Rag1*^{null} *IL2rg*^{null} (NRG) mice with luciferase transduced MV4-11 FLT3-ITD model of adaptive resistance to type II TKIs. Mice were randomised on detection of BLI and treated with vehicle, WSD-0628, sorafenib, quizartinib, or WSD-0628 combined with either sorafenib or quizartinib (Figure 6E-J). After 4 weeks, leukaemia burden (BLI) significantly decreased in mice treated with WSD-0628 alone (p=0.02) and combined with sorafenib (p=0.04), but not with sorafenib alone (Figure 6E-F). Sorafenib monotherapy did not extend survival compared to the vehicle group (59 days vs. 56.5 days) (Figure 6G). Mice treated with WSD-0628 monotherapy survived longer than both the vehicle group (70.5 days vs. 56.5 days, p=0.006) and the sorafenib group (70.5 days vs. 59 days, p=0.02). WSD-0628 combined with sorafenib significantly extended survival compared to the vehicle (68 days vs. 56.5 days, p=0.003) and sorafenib groups (68 days vs. 59 days, p=0.03), but not compared to WSD-0628 monotherapy (68 days vs. 70.5 days) (Figure 6G).

Next, we evaluated the effects of WSD-0628 and quizartinib as monotherapies, and in combination. After 4 weeks, mice treated with WSD-0628 alone (p=0.03) and in combination

with quizartinib (p=0.01) showed a significant reduction in leukaemia burden, whereas those treated with quizartinib alone did not (Figure 6H-I). Quizartinib monotherapy did not extend survival compared to controls (74 vs. 71 days). In contrast, WSD-0628 alone significantly extended survival (86.5 vs. 71 days, p=0.009). The combination of WSD-0628 and quizartinib further extended survival compared to vehicle- (90 vs. 71 days, p=0.0003) and quizartinib-treated groups (90 vs. 74 days, p=0.03), but not significantly compared to WSD-0628 alone (90 vs. 86.5 days) (Figure 6J). After 120 days, 50% of mice treated with the combination showed no signs of leukaemia (Figure 6J).

To assess if ATM inhibition promotes similar responses in *in vivo* models of FLT3-ITD TKI sensitive models MV4-11 FLT3-ITD cell lines were engrafted and treated with vehicle, WSD-0628, or sorafenib (Supplementary Figure S4). After 4 weeks, sorafenib alone significantly reduce leukaemia burden (p=0.0167) compared to vehicle controls. WSD-0628 did not significantly reduce BLI radiance over 4 weeks but stalled leukaemia progression, showing a significant decrease after 5 weeks (p=0.0347) (Supplementary Figure S4A). Sorafenib significantly extended survival (53 vs. 40 days, p=0.0155), as did WSD-0628 monotherapy (55 vs. 40 days, p=0.0006) (Supplementary Figure S4B).

DISCUSSION

The development and approval of TKIs targeting FLT3 have improved treatment strategies for FLT3-ITD AML patients. Currently, two TKIs, midostaurin and quizartinib, are FDA-approved for use with induction chemotherapy in newly diagnosed FLT3-mutant AML. Additionally, sorafenib is often used off-label post allo-HCT or following resistance in relapsed FLT3-ITD AML patients who have also received gilteritinib salvage treatment (16). For the treatment of pAML, sorafenib is the most extensively studied first-generation FLT3 inhibitor (44), with reports showing it can be safely combined with standard of care chemotherapy to improve outcomes in high allelic ratio (HAR) (AR > 0.4) FLT3-ITD pAML (AAML1031) (17).

389 However, relapse following TKIs remains a challenge, and the lack of alternative
390 treatments for patients who only transiently respond to current FLT3-targeted therapies
391 contributes to low survival rates. Here, we present a comprehensive phosphoproteomic
392 analysis of FLT3-ITD AML resistant to type II TKIs, sorafenib and quizartinib. We found that
393 ROS-driven DDR signaling, particularly through ATM regulation, is overactivated in TKI-
394 resistant cells, promoting survival despite treatment. This study identifies key factors
395 controlling TKI-resistant cell survival, providing crucial information for designing patient-
396 specific therapies targeting both common and divergent oncogenic signaling pathways.

397 Our phosphoproteomics analysis revealed that ATM-driven DNA repair signalling is
398 crucial for cell survival and therapy resistance in FLT3-ITD/TKD cells. The DDR pathway,
399 activated by endogenous DNA damage often caused by ROS, is a key factor. High ROS levels
400 drive progression in FLT3-ITD AML (29, 36, 37). We confirmed that TKI-resistant cells produce
401 more ROS than TKI-sensitive cells due to increased NOX2/4 protein expression, indicating a
402 redox imbalance that aids survival. This pattern is also seen in AML patients resistant to SOC
403 (37). Reducing ROS increased the proliferation of resistant cells, suggesting less reliance on
404 DDR response and more energy for proliferation.

405 Acute FLT3 inhibition induces ROS accumulation, activating ATM signalling to
406 maintain redox homeostasis (48). We observed increased phosphorylation of histone H2AX
407 (γH2AX pSer139), ATM (S1981), and DNA-PK (S2609, S2612) kinases in resistant cells,
408 highlighting their role in DDR signalling regulation (45). Inhibiting ATM in TKI-resistant cells
409 significantly increased DNA fragmentation and oxidative DNA damage, which did not occur in
410 TKI-sensitive cells. This underscores the importance of enhanced DNA repair via ATM for cell
411 survival under oxidative stress in TKI-resistance, presenting a novel therapeutic vulnerability
412 in TKI resistance and as a salvage therapy post-TKI failure.

413 In the current clinical management of leukaemia, minimal residual disease (MRD)
414 detection provides critical insight into the remission status of patients and has significantly
415 contributed to the overall improvement in survival rates (46). However, pAML patients with

higher MRD-positive rates after standard induction therapies are at an increased risk of relapse and have worse overall survival (47). Importantly, we identified that pAML patients with high-level expression of ATM fare significantly worse across all disease settings than those with low ATM expression.

Increased activity and expression of NOX enzymes responsible for high oxidative stress in high-risk AML are well-documented, but therapeutic targeting remains challenging (37, 48). Our findings suggest that ROS-mediated ATM signalling drives a constitutive DDR feedback loop that sustains cell survival under ROS-induced stress (38, 48), presenting an exciting therapeutic opportunity. Given the interest in ATM kinase inhibitors across various cancers (49), we evaluated ATM inhibition as a strategy against SOC- and FLT3-ITD/TKD-resistance. Treatment with the clinically relevant ATM inhibitor WSD-0628, alone and in combination, successfully reduced resistant cell proliferation *in vitro* and decreased phosphorylation of ATM kinase and γH2AX, critical for DSB repair fidelity (43). *In vivo*, ATM inhibition reduced leukaemia burden and significantly increased survival of mice engrafted with TKI-resistant cells, either as a single agent or in combination with TKIs sorafenib and quizartinib.

Clinically, WSD-0628 is being tested with radiation therapy for glioblastoma (NCT05917145), and new studies are underway for paediatric diffuse midline gliomas. Our data suggest that ATM inhibition could be a valuable addition to standard induction therapies, used in consolidation, or as a salvage therapy at relapse in R/R FLT3-mutant AML. This approach may address the high MRD-positive rates and poor outcomes associated with high ATM expression, providing a novel and promising therapeutic strategy for improving patient survival.

Word count: 4020

ACKNOWLEDGMENTS

N. Smith from the University of Newcastle Analytical and Biomolecular Research Facility (ABRF) provided MS support. The Academic and Research Computing Support (ARCS) team, within Digital Technology Solutions at the University of Newcastle, provided high-performance computing (HPC) infrastructure supporting bioinformatic analyses.

The ATM inhibitor, WSD-0628, used in this study was supplied by Wayshine Biopharm International Ltd, Corona, California under a materials transfer agreement with the University of Newcastle, Callaghan, Australia.

Funding: This study was supported by Cancer Institute NSW Fellowships (M.D.D., N.M.V., and H.C.M. (ECF1299)). M.D.D., is supported by an NHMRC Investigator grant, GNT1173892. The contents of the published material are solely the responsibility of the research institutions involved or individual authors and do not reflect the views of NHMRC. The ARC provided a Future Fellowship (N.M.V.), HNE/NSW Health Pathology/CMN a Clinical Translational Research Fellowship (A.K.E.). This project is supported by an NHMRC Ideas Grant APP1188400. Additionally, this project was supported by grant 2023/PCRS/0146 awarded through the 2023 Priority-driven Collaborative Cancer Research Scheme and co-funded by Cancer Australia and The Kids' Cancer Project. Grants from the Hunter Medical Research Institute, Hunter Children's Research Foundation, Jurox Animal Health, Zebra Equities, Australian Lions Childhood Cancer Research Foundation, Hunter District Hunting Club and Ski for Kids, and the Estate of James Scott Lawrie supported the research works. and the Cancer Institute NSW in partnership with the College of Health, Medicine and Wellbeing from the University of Newcastle funded the MS platform.

AUTHOR CONTRIBUTIONS

D.E.S., Z.P.G., A.M., T.M. and M.D.D. conceived and designed the study and interpreted the results; D.E.S., Z.P.G., A.M., T.M., L.C., G.D.I., and M.D.D. conducted the experiments and performed data analysis; B.C.T., H.P.M., H.C.M., R.J.D., T.B., M.L.P., I.J.F., E.R.J., N.D.S., D.A.S., B.N., and N.V. helped with experimental work and/or interpretation of results; P.C.,

assisted with bioinformatic analyses; D.M., W.J., A.K.E., J.R.S., J.C., F.A. provided discipline-specific expertise; J.C., F.A., J.R.S., A.K.E., and A.H.W. assisted with obtaining and processing of patient samples; D.E.S., Z.P.G., A.M.D., and M.D.D. wrote and edited the manuscript; and all authors discussed the results and commented on the manuscript.

Data and materials availability: MTA agreements and publicly accessible data as described in Materials and Methods.

REFERENCES

1. Staudt D, Murray HC, McLachlan T, Alvaro F, Enjeti AK, Verrills NM, Dun MD. Targeting Oncogenic Signaling in Mutant FLT3 Acute Myeloid Leukemia: The Path to Least Resistance. Int J Mol Sci. 2018 Oct 16;19(10). Epub 2018/10/20. doi:10.3390/ijms19103198. Cited in: Pubmed; PMID 30332834.

2. Yanada M, Matsuo K, Suzuki T, Kiyoi H, Naoe T. Prognostic significance of FLT3 internal tandem duplication and tyrosine kinase domain mutations for acute myeloid leukemia: a meta-analysis. Leukemia. 2005 Aug;19(8):1345-9. eng. doi:10.1038/sj.leu.2403838. Cited in: Pubmed; PMID 15959528.

3. Thiede C, Steudel C, Mohr B, Schaich M, Schäkel U, Platzbecker U, Wermke M, Bornhäuser M, Ritter M, Neubauer A, Ehninger G, Illmer T. Analysis of FLT3-activating mutations in 979 patients with acute myelogenous leukemia: association with FAB subtypes and identification of subgroups with poor prognosis. Blood. 2002 Jun 15;99(12):4326-35. eng. doi:10.1182/blood.v99.12.4326. Cited in: Pubmed; PMID 12036858.

4. Verstraete K, Savvides SN. Extracellular assembly and activation principles of oncogenic class III receptor tyrosine kinases. Nat Rev Cancer. 2012 Nov;12(11):753-66. eng. Epub 20121018. doi:10.1038/nrc3371. Cited in: Pubmed; PMID 23076159.

5. Zhang S, Mantel C, Broxmeyer HE. Flt3 signaling involves tyrosyl-phosphorylation of SHP-2 and SHIP and their association with Grb2 and Shc in Baf3/Flt3 cells. J Leukoc Biol. 1999 Mar;65(3):372-80. eng. doi:10.1002/jlb.65.3.372. Cited in: Pubmed; PMID 10080542.

6. Zhang S, Fukuda S, Lee Y, Hangoc G, Cooper S, Spolski R, Leonard WJ, Broxmeyer HE. Essential role of signal transducer and activator of transcription (Stat)5a but not Stat5b for Flt3-dependent signaling. J Exp Med. 2000 Sep 4;192(5):719-28. eng. doi:10.1084/jem.192.5.719. Cited in: Pubmed; PMID 10974037.

7. Zhang S, Broxmeyer HE. Flt3 ligand induces tyrosine phosphorylation of gab1 and gab2 and their association with shp-2, grb2, and PI3 kinase. Biochem Biophys Res Commun. 2000 Oct 14;277(1):195-9. eng. doi:10.1006/bbrc.2000.3662. Cited in: Pubmed; PMID 11027663.

8. Kihara R, Nagata Y, Kiyoi H, Kato T, Yamamoto E, Suzuki K, Chen F, Asou N, Ohtake S, Miyawaki S, Miyazaki Y, Sakura T, Ozawa Y, Usui N, Kanamori H, Kiguchi T, Imai K, Uike N, Kimura F, Kitamura K, Nakaseko C, Onizuka M, Takeshita A, Ishida F, Suzushima H, Kato Y, Miwa H, Shiraishi Y, Chiba K, Tanaka H, Miyano S, Ogawa S, Naoe T. Comprehensive analysis of genetic alterations and their prognostic impacts in adult acute myeloid leukemia patients. Leukemia. 2014 Aug;28(8):1586-95. eng. Epub 20140203. doi:10.1038/leu.2014.55. Cited in: Pubmed; PMID 24487413.

9. Yamamoto Y, Kiyoi H, Nakano Y, Suzuki R, Kodera Y, Miyawaki S, Asou N, Kuriyama K, Yagasaki F, Shimazaki C, Akiyama H, Saito K, Nishimura M, Motoji T, Shinagawa K, Takeshita A, Saito H, Ueda R, Ohno R, Naoe T. Activating mutation of D835 within the activation loop of FLT3 in human hematologic malignancies. Blood. 2001 Apr 15;97(8):2434-9. eng. doi:10.1182/blood.v97.8.2434. Cited in: Pubmed; PMID 11290608.

10. Zhao JC, Agarwal S, Ahmad H, Amin K, Bewersdorf JP, Zeidan AM. A review of FLT3 inhibitors in acute myeloid leukemia. Blood Reviews. 2022 2022/03/01/;52:100905. doi:https://doi.org/10.1016/j.blre.2021.100905.

11. Larrosa-Garcia M, Baer MR. FLT3 Inhibitors in acute myeloid leukemia: Current status & future directions. Molecular Cancer Therapeutics. 2017;16(6):991-1001. doi:10.1158/1535-7163.MCT-16-0876.

12. Friedman R. The molecular mechanisms behind activation of FLT3 in acute myeloid leukemia and resistance to therapy by selective inhibitors. Biochim Biophys Acta Rev Cancer. 2022 Jan;1877(1):188666. eng. Epub 20211208. doi:10.1016/j.bbcan.2021.188666. Cited in: Pubmed; PMID 34896257.

13. Stone RM, Mandrekar SJ, Sanford BL, Laumann K, Geyer S, Bloomfield CD, Thiede C, Prior TW, Döhner K, Marcucci G, Lo-Coco F, Klisovic RB, Wei A, Sierra J, Sanz MA, Brandwein JM, de Witte T, Niederwieser D, Appelbaum FR, Medeiros BC, Tallman MS, Krauter J, Schlenk RF, Ganser A, Serve H, Ehninger G, Amadori S, Larson RA, Döhner H. Midostaurin plus Chemotherapy for Acute Myeloid Leukemia with a FLT3 Mutation. N Engl J Med. 2017 Aug 3;377(5):454-464. eng. Epub 20170623. doi:10.1056/NEJMoa1614359. Cited in: Pubmed; PMID 28644114.

14. Erba HP, Montesinos P, Kim HJ, Patkowska E, Vrhovac R, Žák P, Wang PN, Mitov T, Hanyok J, Kamel YM, Rohrbach JEC, Liu L, Benzohra A, Lesegretain A, Cortes J, Perl AE, Sekeres MA, Dombret H, Amadori S, Wang J, Levis MJ, Schlenk RF. Quizartinib plus chemotherapy in newly diagnosed patients with FLT3-internal-tandem-duplication-positive acute myeloid leukaemia (QuANTUM-First): a randomised, double-blind, placebo-controlled, phase 3 trial. Lancet. 2023 May 13;401(10388):1571-1583. eng. Declaration of interests HPE reports research grants from AbbVie, Agios Pharmaceuticals, ALX Oncology, Amgen, Ascentage, Celgene, Daiichi Sankyo, Forma Therapeutics, Forty Seven, Gilead, GlycoMimetics, ImmunoGen, Jazz Pharmaceuticals, Kura Oncology, MacroGenics, Novartis, PTC Therapeutics, Servier, and Sumitomo Dainippon Pharma; consulting fees for participation on advisory boards for AbbVie, Agios Pharmaceuticals, Astellas, Bristol Myers Squibb, Celgene, Daiichi Sankyo, Genentech, GlycoMimetics, ImmunoGen, Incyte, Jazz Pharmaceuticals, Kura Oncology, MacroGenics, Novartis, Pfizer, Servier, Syros Pharmaceuticals, Takeda, and Trillium Therapeutics; payment for speakers bureaus from AbbVie, Agios Pharmaceuticals, Bristol Myers Squibb, Celgene, Incyte, Jazz Pharmaceuticals, Novartis, and Servier; and has served as a steering committee member for GlycoMimetics, as chair of the Myeloid Neoplasms Repository study for Bristol Myers Squibb and Celgene, and as chair of the independent review committee of the VIALE A and VIALE C studies for AbbVie. PM reports research grants from AbbVie, Bristol Myers Squibb, Jazz Pharmaceuticals, Menarini, Stemline Therapeutics, Novartis, Pfizer, and Takeda; consulting fees from AbbVie, Astellas, BeiGene, Bristol Myers Squibb, Gilead, Incyte, Jazz Pharmaceuticals, Kura Oncology, Menarini, Stemline Therapeutics, Nerviano Medical Sciences, Novartis, Otsuka Pharmaceutical, Pfizer, Ryvu Therapeutics, and Takeda; and payment for speakers bureaus from AbbVie, Astellas, Bristol Myers Squibb, Gilead, Jazz Pharmaceuticals, and Pfizer. H-JK reports research grants from BL&H; consulting fees from AbbVie, AIMS BioScience, Amgen, AMLHub, Astellas, Aston BioSciences, Bristol Myers Squibb, Celgene, Boryung Pharmaceutical, Daiichi Sankyo, Handok, Ingenium, Janssen, LG Chem, Novartis, Pfizer, Sanofi Genzyme, SL VaxiGen, and VigenCell; is on a data safety monitoring board or advisory board for AbbVie, the Asia Pacific Leukemia Consortium, Astellas, Bristol Myers Squibb, Celgene, Daiichi Sankyo, Handok, Janssen, Novartis, Pfizer, and Sanofi Genzyme; and is a leader in other board, society, committee, or advocacy groups for AMLHub, the Asia Pacific Leukemia

Consortium, the Asia Pacific Blood and Marrow Transplantation Group, and the Korean Society of Blood and Marrow Transplantation. EP reports consulting fees from KCR US; payment for lectures from Amgen, Angelini, Astellas, Novartis, Pfizer, and Servier; and support for attending meetings from Angelini, Astellas, Bristol Myers Squibb, Jazz Pharmaceuticals, Novartis, Pfizer, and Servier. RV reports consulting fees from AbbVie, Astellas, Pfizer, and PharmaS; and payment for lectures from AbbVie, Astellas, Merck Sharp & Dohme, Novartis, Pfizer, PharmaS, Servier, and Teva. JC reports research grants from AbbVie, Daiichi Sankyo, Novartis, Sun Pharma, and Pfizer; consulting fees from AbbVie, Bio-Path, Daiichi Sankyo, Gilead, Forma Therapeutics, Novartis, Pfizer, and Takeda; payment for lectures from Novartis, Pfizer, and Takeda; and has stock options with Bio-Path. AEP reports research grants from AbbVie, Actinium Pharmaceuticals, Astellas, Bayer, BioMed Valley Discoveries, and Daiichi Sankyo; personal fees from Actinium Pharmaceuticals, Agios Pharmaceuticals, Astellas, Daiichi Sankyo, Forma Therapeutics, Jazz Pharmaceuticals, Leukemia & Lymphoma Society (Beat AML Master Clinical Trial), Loxo Oncology, NewLink Genetics, Novartis, and Takeda; and non-financial support from Arog Pharmaceuticals, Astellas, Jazz Pharmaceuticals, NewLink Genetics, Novartis, and Takeda. MAS reports consulting fees from Bristol Myers Squibb, Kurome Therapeutics, and Novartis; and has stock options with Kurome Therapeutics. HD reports personal fees from Incyte and Servier. JW reports payment for participation on an advisory board from Abbvie and for participation on a data safety monitoring committee from AstraZeneca. MJL reports research grants from Astellas and FujiFilm Pharmaceuticals; consulting fees from AbbVie, Amgen, Bristol Myers Squibb, Daiichi Sankyo, Jazz Pharmaceuticals, Menarini, Pfizer, and Takeda; and payment for lectures from Astellas. RFS reports consulting fees from Daiichi Sankyo for participation on a steering committee and from AbbVie, Jazz Pharmaceuticals, and Pfizer for participation on advisory boards; payment for lectures from Daiichi Sankyo, Novartis, and Pfizer; is on a data safety monitoring board or advisory board for BerGenBio and Novartis; and has been provided with equipment by AbbVie, AstraZeneca, Boehringer Ingelheim, Daiichi Sankyo, PharmaMar, Pfizer, and Roche. TM, JH, YMK, JECR, LL, AB, and AL are employees of Daiichi Sankyo. All other authors declare no competing interests. Epub 20230425. doi:10.1016/s0140-6736(23)00464-6. Cited in: Pubmed; PMID 37116523.

15. Dhillon S. Gilteritinib: First Global Approval. Drugs. 2019 Feb;79(3):331-339. eng. doi:10.1007/s40265-019-1062-3. Cited in: Pubmed; PMID 30721452.

16. Antar AI, Otrock ZK, Jabbour E, Mohty M, Bazarbachi A. FLT3 inhibitors in acute myeloid leukemia: ten frequently asked questions. Leukemia. 2020 Mar;34(3):682-696. eng. Epub 20200109. doi:10.1038/s41375-019-0694-3. Cited in: Pubmed; PMID 31919472.

17. Pollard JA, Alonzo TA, Gerbing R, Brown P, Fox E, Choi J, Fisher B, Hirsch B, Kahwash S, Getz K, Levine J, Brodersen LE, Loken MR, Raimondi S, Tarlock K, Wood A, Sung L, Kolb EA, Gamis A, Meshinchi S, Aplenc R. Sorafenib in Combination With Standard Chemotherapy for Children With High Allelic Ratio FLT3/ITD+ Acute Myeloid Leukemia: A Report From the Children's Oncology Group Protocol AAML1031. J Clin Oncol. 2022 Jun 20;40(18):2023-2035. eng. Jessica A. PollardConsulting or Advisory Role: Syndax, Kura Oncology Patrick BrownConsulting or Advisory Role: Novartis, Jazz Pharmaceuticals, Servier, Kite, a Gilead company, Amgen, Kura Oncology, Takeda Brian FisherConsulting or Advisory Role: Astellas PharmaResearch Funding: Pfizer (Inst), Merck (Inst) John LevineConsulting or Advisory Role: Talaris, Bluebird Bio, Mesoblast, Therakos, SymBio Pharmaceuticals, X4 Pharmaceuticals, Equillium, Jazz Pharmaceuticals, OncoImmune, OmerosResearch Funding: Incyte (Inst), Kamada (Inst), Biogen (Inst), Mesoblast (Inst), MaaT Pharmaceuticals (Inst)Patents, Royalties, Other Intellectual Property: GVHD biomarkers patent licensed to VIracor Lisa Eidenschink BrodersenEmployment: Hematologics IncLeadership: Hematologics Inc Michael R. LokenEmployment: Hematologics IncLeadership: Hematologics IncStock and Other Ownership Interests: Hematologics IncConsulting or Advisory Role: Newlink Genetics

Andrew WoodPatents, Royalties, Other Intellectual Property: PAT055863-US-PCT. Inventor assigned to Genomics Institute of the Novartis Research Foundation involving combination inhibition of ALK, PAT055863-US-PCT. Inventor assigned to Genomics Institute of the Novartis Research Foundation involving combination inhibition of ALK E. Anders KolbTravel, Accommodations, Expenses: Roche/Genentech Lillian SungThis author is a member of the Journal of Clinical Oncology Editorial Board. Journal policy recused the author from having any role in the peer review of this manuscript. Alan GamisConsulting or Advisory Role: Novartis Richard AplencExpert Testimony: VorysNo other potential conflicts of interest were reported. Epub 20220329. doi:10.1200/jco.21.01612. Cited in: Pubmed; PMID 35349331.

18. Sato T, Yang X, Knapper S, White P, Smith BD, Galkin S, Small D, Burnett A, Levis M. FLT3 ligand impedes the efficacy of FLT3 inhibitors in vitro and in vivo. Blood. 2011;117(12):3286-3293. doi:10.1182/blood-2010-01-266742.

19. Ding L, Ley TJ, Larson DE, Miller CA, Koboldt DC, Welch JS, Ritchey JK, Young MA, Lamprecht T, McLellan MD, McMichael JF, Wallis JW, Lu C, Shen D, Harris CC, Dooling DJ, Fulton RS, Fulton LL, Chen K, Schmidt H, Kalicki-Veizer J, Magrini VJ, Cook L, McGrath SD, Vickery TL, Wendl MC, Heath S, Watson MA, Link DC, Tomasson MH, Shannon WD, Payton JE, Kulkarni S, Westervelt P, Walter MJ, Graubert TA, Mardis ER, Wilson RK, DiPersio JF. Clonal evolution in relapsed acute myeloid leukaemia revealed by whole-genome sequencing. Nature. 2012 2012/01/01;481(7382):506-510. doi:10.1038/nature10738.

20. Ghiaur G, Levis M. Mechanisms of Resistance to FLT3 Inhibitors and the Role of the Bone Marrow Microenvironment. Hematology/Oncology Clinics of North America. 2017 2017/08/01/;31(4):681-692. doi:https://doi.org/10.1016/j.hoc.2017.04.005.

21. Park IK, Mundy-Bosse B, Whitman SP, Zhang X, Warner SL, Bearss DJ, Blum W, Marcucci G, Caligiuri MA. Receptor tyrosine kinase Axl is required for resistance of leukemic cells to FLT3-targeted therapy in acute myeloid leukemia. Leukemia. 2015 2015/12/01;29(12):2382-2389. doi:10.1038/leu.2015.147.

22. von Bubnoff N, Engh RA, Aberg E, Sänger J, Peschel C, Duyster J. FMS-like tyrosine kinase 3-internal tandem duplication tyrosine kinase inhibitors display a nonoverlapping profile of resistance mutations in vitro. Cancer Res. 2009 Apr 1;69(7):3032-41. eng. Epub 20090324. doi:10.1158/0008-5472.Can-08-2923. Cited in: Pubmed; PMID 19318574.

23. Williams AB, Nguyen B, Li L, Brown P, Levis M, Leahy D, Small D. Mutations of FLT3/ITD confer resistance to multiple tyrosine kinase inhibitors. Leukemia. 2013 2013/01/01;27(1):48-55. doi:10.1038/leu.2012.191.

24. Smith CC, Lin K, Stecula A, Sali A, Shah NP. FLT3 D835 mutations confer differential resistance to type II FLT3 inhibitors. Leukemia. 2015 Dec;29(12):2390-2. eng. Epub 20150625. doi:10.1038/leu.2015.165. Cited in: Pubmed; PMID 26108694.

25. Dun MD, Mannan A, Rigby CJ, Butler S, Toop HD, Beck D, Connerty P, Sillar J, Kahl RGS, Duchatel RJ, Germon Z, Faulkner S, Chi M, Skerrett-Byrne D, Murray HC, Flanagan H, Almazi JG, Hondermarck H, Nixon B, De Iuliis G, Chamberlain J, Alvaro F, de Bock CE, Morris JC, Enjeti AK, Verrills NM.

Shwachman-Bodian-Diamond syndrome (SBDS) protein is a direct inhibitor of protein phosphatase 2A (PP2A) activity and overexpressed in acute myeloid leukaemia. Leukemia. 2020 Dec;34(12):3393-3397. The authors declare that they have no conflict of interest. Epub 20200408. doi:10.1038/s41375-020-0814-0. Cited in: Pubmed; PMID 32269318.

26. Staudt DE, Murray HC, Skerrett-Byrne DA, Smith ND, Jamaluddin MFB, Kahl RGS, Duchatel RJ, Germon ZP, McLachlan T, Jackson ER, Findlay IJ, Kearney PS, Mannan A, McEwen HP, Douglas AM, Nixon B, Verrills NM, Dun MD. Phospho-heavy-labeled-spiketide FAIMS stepped-CV DDA (pHASED) provides real-time phosphoproteomics data to aid in cancer drug selection. Clin Proteomics. 2022 Dec 19;19(1):48. The authors have no conflicts of interest to report. Epub 20221219. doi:10.1186/s12014-022-09385-7. Cited in: Pubmed; PMID 36536316.

27. Perez-Riverol Y, Bai J, Bandla C, García-Seisdedos D, Hewapathirana S, Kamatchinathan S, Kundu DJ, Prakash A, Frericks-Zipper A, Eisenacher M, Walzer M, Wang S, Brazma A, Vizcaíno JA. The PRIDE database resources in 2022: a hub for mass spectrometry-based proteomics evidences. Nucleic Acids Res. 2022 Jan 7;50(D1):D543-d552. eng. doi:10.1093/nar/gkab1038. Cited in: Pubmed; PMID 34723319.

28. Grossman RL, Heath AP, Ferretti V, Varmus HE, Lowy DR, Kibbe WA, Staudt LM. Toward a Shared Vision for Cancer Genomic Data. N Engl J Med. 2016 Sep 22;375(12):1109-12. doi:10.1056/NEJMp1607591. Cited in: Pubmed; PMID 27653561.

29. Germon ZP, Sillar JR, Mannan A, Duchatel RJ, Staudt D, Murray HC, Findlay IJ, Jackson ER, McEwen HP, Douglas AM, McLachlan T, Schjenken JE, Skerrett-Byrne DA, Huang H, Melo-Braga MN, Plank MW, Alvaro F, Chamberlain J, De Iuliis G, Aitken RJ, Nixon B, Wei AH, Enjeti AK, Huang Y, Lock RB, Larsen MR, Lee H, Vaghjiani V, Cain JE, de Bock CE, Verrills NM, Dun MD. Blockade of ROS production inhibits oncogenic signaling in acute myeloid leukemia and amplifies response to precision therapies. Sci Signal. 2023 Mar 28;16(778):eabp9586. Epub 20230328. doi:10.1126/scisignal.abp9586. Cited in: Pubmed; PMID 36976863.

30. De Iuliis GN, Newey RJ, King BV, Aitken RJ. Mobile Phone Radiation Induces Reactive Oxygen Species Production and DNA Damage in Human Spermatozoa In Vitro. PLOS ONE. 2009;4(7):e6446. doi:10.1371/journal.pone.0006446.

31. Griffith J, Black J, Faerman C, Swenson L, Wynn M, Lu F, Lippke J, Saxena K. The Structural Basis for Autoinhibition of FLT3 by the Juxtamembrane Domain. Molecular Cell. 2004;13(2):169-178. doi:10.1016/S1097-2765(03)00505-7.

32. Kazi JU, Rönnstrand L. Tyrosine 842 Residue in the Activation Loop of FLT3-ITD Is Indespensible for Oncogenic Transformation. Blood. 2016;128(22):1561-1561. doi:10.1182/blood.V128.22.1561.1561.

33. Murray HC, Enjeti AK, Kahl RGS, Flanagan HM, Sillar J, Skerrett-Byrne DA, Al Mazi JG, Au GG, de Bock CE, Evans K, Smith ND, Anderson A, Nixon B, Lock RB, Larsen MR, Verrills NM, Dun MD. Quantitative phosphoproteomics uncovers synergy between DNA-PK and FLT3 inhibitors in acute myeloid leukaemia. Leukemia. 2021 2021/06/01;35(6):1782-1787. doi:10.1038/s41375-020-01050-y.

34. Dasika GK, Lin S-CJ, Zhao S, Sung P, Tomkinson A, Lee EYHP. DNA damage-induced cell cycle checkpoints and DNA strand break repair in development and tumorigenesis. Oncogene. 1999 1999/12/01;18(55):7883-7899. doi:10.1038/sj.onc.1203283.

35. Shiloh Y, Ziv Y. The ATM protein kinase: regulating the cellular response to genotoxic stress, and more. Nature Reviews Molecular Cell Biology. 2013 2013/04/01;14(4):197-210. doi:10.1038/nrm3546.

36. Sallmyr A, Fan J, Datta K, Kim KT, Grosu D, Shapiro P, Small D, Rassool F. Internal tandem duplication of FLT3 (FLT3/ITD) induces increased ROS production, DNA damage, and misrepair: implications for poor prognosis in AML. Blood. 2008 Mar 15;111(6):3173-82. eng. Epub 20080111. doi:10.1182/blood-2007-05-092510. Cited in: Pubmed; PMID 18192505.

37. Sillar JR, Germon ZP, DeIuliis GN, Dun MD. The Role of Reactive Oxygen Species in Acute Myeloid Leukaemia. Int J Mol Sci. 2019 Nov 28;20(23). Epub 2019/12/05. doi:10.3390/ijms20236003. Cited in: Pubmed; PMID 31795243.

38. Gregory MA, D'Alessandro A, Alvarez-Calderon F, Kim J, Nemkov T, Adane B, Rozhok AI, Kumar A, Kumar V, Pollyea DA, Wempe MF, Jordan CT, Serkova NJ, Tan AC, Hansen KC, DeGregori J. ATM/G6PD-driven redox metabolism promotes FLT3 inhibitor resistance in acute myeloid leukemia. Proc Natl Acad Sci U S A. 2016 Oct 25;113(43):E6669-e6678. eng. The authors declare no conflict of interest. Epub 20161010. doi:10.1073/pnas.1603876113. Cited in: Pubmed; PMID 27791036.

39. Hole PS, Zabkiewicz J, Munje C, Newton Z, Pearn L, White P, Marquez N, Hills RK, Burnett AK, Tonks A, Darley RL. Overproduction of NOX-derived ROS in AML promotes proliferation and is associated with defective oxidative stress signaling. Blood. 2013 Nov 7;122(19):3322-30. Epub 20131002. doi:10.1182/blood-2013-04-491944. Cited in: Pubmed; PMID 24089327.

40. Eklund EA, Kakar R. Recruitment of CREB-binding protein by PU.1, IFN-regulatory factor-1, and the IFN consensus sequence-binding protein is necessary for IFN-gamma-induced p67phox and gp91phox expression. J Immunol. 1999 Dec 1;163(11):6095-105. eng. Cited in: Pubmed; PMID 10570299.

41. BLISS CI. THE TOXICITY OF POISONS APPLIED JOINTLY1. Annals of Applied Biology. 1939;26(3):585-615. doi:https://doi.org/10.1111/j.1744-7348.1939.tb06990.x.

42. White D, Rafalska-Metcalf IU, Ivanov AV, Corsinotti A, Peng H, Lee SC, Trono D, Janicki SM, Rauscher FJ, 3rd. The ATM substrate KAP1 controls DNA repair in heterochromatin: regulation by HP1 proteins and serine 473/824 phosphorylation. Mol Cancer Res. 2012 Mar;10(3):401-14. eng. Epub 20111228. doi:10.1158/1541-7786.Mcr-11-0134. Cited in: Pubmed; PMID 22205726.

43. Scully R, Xie A. Double strand break repair functions of histone H2AX. Mutation Research/Fundamental and Molecular Mechanisms of Mutagenesis. 2013 2013/10/01/;750(1):5-14. doi:https://doi.org/10.1016/j.mrfmmm.2013.07.007.

758 44. Lonetti A, Pession A, Masetti R. Targeted Therapies for Pediatric AML: Gaps and Perspective
759 [Review]. Frontiers in Pediatrics. 2019;7.

760

761 45. Stracker TH, Roig I, Knobel PA, Marjanović M. The ATM signaling network in development and
762 disease. Front Genet. 2013;4:37. eng. Epub 20130325. doi:10.3389/fgene.2013.00037. Cited in:
763 Pubmed; PMID 23532176.

764

765 46. McLachlan T, Matthews WC, Jackson ER, Staudt DE, Douglas AM, Findlay IJ, Persson ML, Duchatel
766 RJ, Mannan A, Germon ZP, Dun MD. B-cell Lymphoma 6 (BCL6): From Master Regulator of Humoral
767 Immunity to Oncogenic Driver in Pediatric Cancers. Mol Cancer Res. 2022 Dec 2;20(12):1711-1723.
768 doi:10.1158/1541-7786.MCR-22-0567. Cited in: Pubmed; PMID 36166198.

769

770 47. Gamis AS, Alonzo TA, Perentesis JP, Meshinchi S, Committee COGAML. Children's Oncology
771 Group's 2013 blueprint for research: acute myeloid leukemia. Pediatr Blood Cancer. 2013
772 Jun;60(6):964-71. Epub 2012/12/21. doi:10.1002/pbc.24432. Cited in: Pubmed; PMID 23255301.

773

774 48. Mannan A, Germon ZP, Chamberlain J, Sillar JR, Nixon B, Dun MD. Reactive Oxygen Species in
775 Acute Lymphoblastic Leukaemia: Reducing Radicals to Refine Responses. Antioxidants (Basel). 2021
776 Oct 14;10(10). The authors declare no conflict of interest. Epub 20211014.
777 doi:10.3390/antiox10101616. Cited in: Pubmed; PMID 34679751.

778

779 49. Lavin MF, Yeo AJ. Clinical potential of ATM inhibitors. Mutation Research/Fundamental and
780 Molecular Mechanisms of Mutagenesis. 2020 2020/05/01/;821:111695.
781 doi:https://doi.org/10.1016/j.mrfmmm.2020.111695.

782

783 **FIGURE LEGENDS**

784 **Figure 1. Comparison of tyrosine kinase inhibitor (TKI) sensitivity of MV4-11 FLT3-ITD**
785 **cell lines.** (A-D) Drug-response for FLT3-ITD sensitive and FLT3-ITD resistant cell lines was
786 assessed using resazurin cell proliferation assays and area under the curve (AUC) was
787 calculated and compared following treatment with type I and type II TKIs as single agents.
788 Treatment with type II TKIs (A) sorafenib and (B) quizartinib confirmed FLT3-ITD adaptive
789 resistance, whereas sensitivity was maintained following treatment with type I TKIs (C)
790 midostaurin, and (D) crenolanib. Cell proliferation was assessed by resazurin fluorescence
791 following 48-hour treatment (unpaired t-test with Welch's correction; n=3 independent
792 biological replicates). (E) Apoptosis and cell death was assessed via Annexin V/PI assay
793 following 48-hour treatment with TKI's as single agents in FLT3-ITD sensitive and FLT3-ITD
794 resistant cell lines. Viable cells (Annexin V/PI negative) plotted as mean +/- SEM (ordinary

one-way ANOVA; n=3 independent biological replicates). (F) Representative FACS image analysis indicating differences in cell death (PI) and apoptosis (Annexin V) after 48-hour treatment with Type I or II TKIs. Significance threshold of *p<0.05, **p<0.01 and ***p<0.001

Figure 2. Structural features of active and inactive FLT3/TKD conformations and consequences for TKI binding. (A) A composite schematic of the FLT3 dimer bound to its ligand (FLT3L) (extracellular domain - PDB: 3QS9, transmembrane and TKD – AF-P36888-F1). (B) Structural overlay of the predicted active conformation for the FLT3 activation loop induced by the ITD mutation, highlighting differential locations of D835 (purple) and Y842 (green) residues with respect to the binding locations of sorafenib. Orange represents the active loop conformation whereas the inactive conformation is highlighted in yellow. (C) Active TKD confirmation demonstrating preferred docking poses of sorafenib and quizartinib. Both D835 (purple) and Y842 (green) residues, in the active confirmation, can influence the binding pocket. (D) Docking poses of sorafenib in both the active (black) and inactive (pink) FLT3-TKD conformations. The presence of D835 and Y842 mutations compromises the stability of the inactive TKD1 conformation, promoting activation. In the activated conformation, F855 (represented by the orange sphere) blocks the ability for sorafenib to anchor in its deep cleft (pink), causing it to bind superficially in the ATP pocket region (black). (E) Binding scores (ChemPLP) of type II TKI's quizartinib and sorafenib to discreet double mutant FLT3 receptor models (higher score = better fit). Cell lines used throughout are indicated by green highlight (MV4-11 resistant) and pink highlight (MV4-11 sensitive).

Figure 3. Phosphoproteomic analysis reveals overactivation of DNA damage and repair (DDR) signalling in FLT3-ITD resistant cells. (A) Identification of two independent phosphosite clusters in resistance. Heatmap (left) and cluster profile (right) of the precursor ion abundances for significantly up/down regulated phosphosites in three independent replicates ($\log_2$ ±0.5; p≤0.05). Yellow represents increased phosphorylation, whereas blue indicates phosphorylation is decreased in TKI resistant cells. (B) Molecular and cellular functions identified by Ingenuity Pathway Analysis (IPA) have been assigned to each cluster

if significantly over-represented by phosphopeptides. (C) DNA damage and repair (DDR) canonical pathways identified by IPA as significantly associated with phosphorylation changes seen in FLT3-ITD resistant cells compared to sensitive cell lines. (D) Activity prediction for DDR kinases based on phosphorylation changes in substrates identified by Kinase-Substrate Enrichment Analysis (KSEA). (E) Protein-protein interaction network for DDR kinases identified by KSEA with a positive z-score in resistance (https://string-db.org/). (F) Western blot analysis further validated the increased expression and phosphorylation of DNA-PK (S2612), ATM (S1981), p53 (S392), and phospho-H2AX (S139) in resistance. (G) Phospho-H2AX (S139) western blotting data was quantified using Image Lab software and presented as a column graph comparing mean values ± SEM (n=3 independent biological replicates). Data was analysed by unpaired Student's t-test. (H) Phosphorylation changes in key DDR signalling proteins identified by mass spectrometry. Values correspond to median $\log_2$ fold change in FLT3-ITD resistant cells compared to FLT3-ITD sensitive cell lines ($\log_2$ ±0.5; n=3 independent biological replicates). (I) Cell number based on relative cell count of FLT3-ITD sensitive (pink) and FLT3-ITD resistant (green) cell lines. Values at timepoints 0-, 24-, and 48-hours are shown (n=3 independent biological replicates). (J) Comparison of growth advantages of FLT3-ITD sensitive and FLT3-ITD resistant cell lines based on 48-hour fold change in cell density relative to day 0. Mean of triplicates ± SEM are shown. (K) Flow cytometry cell cycle analysis after staining with propidium iodide (PI). Cell cycle phase distribution shows the percentage of FLT3-ITD sensitive and FLT3-ITD resistant cells in the G0/G1, S, and G2/M phases of cell cycle at 24-, 48-, and 72-hour timepoints (n=3 independent biological replicates). Representative histogram of cell cycle profiles at 24-hours. Mean of triplicates ± SEM are shown. Significance threshold of *p<0.05, **p<0.01 and ***p<0.001.

Figure 4. Analysis of publicly available survival and expression data stratifies patients based on ATM expression. (A) Patient data from BEAT AML Vizome database were downloaded and expression values (TPM) as well as clinical information were obtained for 68 FLT3-ITD adult AML patients. Patients were separated into high and low ATM expression as

849 determined by TPM value where high expression referred to the top 25% of patients and low
850 expression the bottom 25% of patients (Q1/Q4 split). Survival analysis was then performed
851 using the Kaplan-Meier model and the Log-rank, Mantel-Cox statistical test used to compare
852 overall survival at diagnosis. Next, the Therapeutically Applicable Research to Generate
853 Effective Treatments (TARGET) initiative, phs000465, was downloaded and again expression
854 values (TPM) as well as clinical information were obtained for 285 paediatric AML patients.
855 (B) Event free survival and (C) overall survival in all paediatric AML (pAML) cases, and (D)
856 overall survival in the relapse setting. (E) ATM expression (Log_2 TPM) was then compared
857 across all AML patients from the TARGET database segregated by diagnosis or relapse
858 subtype. Students t-test was performed for statistical comparison. (F) Resazurin proliferation
859 (percentage compared to untreated) assays of FLT3-ITD sensitive and FLT3-ITD DNR
860 (daunorubicin) and Ara-C (cytarabine) resistant cell lines after 48-hour exposure to 25 μM
861 AraC or 250 nM WSD-0628 (minimum of n=3 independent biological replicates). Significance
862 threshold of *p<0.05, **p<0.01 and ***p<0.001 (Two-Way ANOVA).

863 **Figure 5. FLT3-ITD resistant cells display higher levels of reactive oxygen species**
864 **(ROS) in comparison to FLT3-ITD sensitive cell lines.** (A) Flow cytometry histogram
865 overlay of cytoplasmic ROS (superoxide) levels in FLT3-ITD sensitive (pink), and FLT3-ITD
866 resistant (green) cell lines. ROS levels were assessed by DHE-PE fluorescence and analysed
867 using FlowJo software. (B) Geometric means were used for ROS quantification and fold
868 change comparison, presented as a column graph as mean values ± SEM (n=3 independent
869 biological replicates). (C) Analysis of cell proliferation for FLT3-ITD sensitive and FLT3-ITD
870 resistant cells in increasing concentrations of ROS scavenger NAC. Cell proliferation was
871 assessed by resazurin assay following 48-hour treatment (n=3 independent biological
872 replicates). Mean of triplicates ± SEM are shown. (D) ROS-associated canonical pathways
873 identified by Ingenuity Pathway Analysis (IPA) as significantly associated with phosphorylation
874 changes seen in FLT3-ITD resistant cells compared to FLT3-ITD sensitive cell lines. (E)
875 Phosphorylation changes in NOX2 transcription factors ELF1 and IRF8 in FLT3-ITD resistant

cells compared to FLT3-ITD sensitive. (F) Western blotting reveals increased protein expression of NADPH oxidase isoforms NOX2 and NOX4 in resistance. (G) ICC quantification of DNA fragmentation (TUNEL-positive) in FLT3-ITD sensitive and FLT3-ITD resistant cells in untreated conditions and after 48-hours treatment with 250 nM of the ATM inhibitor WSD-0628. (H) ICC quantification of oxidative DNA damage (8-OHdG-positive) in FLT3-ITD sensitive and FLT3-ITD resistant cells carrying knockdown (K.D) of ATM, scramble control or treated for 48-hour with 250 nM WSD-0628. Significance threshold of *p<0.05, **p<0.01 and ***p<0.001 (n=3 independent biological replicates).

Figure 6. Sensitivity to ATM inhibition alone and in combination with FLT3 inhibitors. Resazurin proliferation (percentage compared to untreated) of FLT3-ITD resistant cell lines after 48-hour exposure to WSD-0628 alone, and in combination with FLT3 inhibitors (A) sorafenib and (B) quizartinib. Values shown as mean ± SEM (n=3 independent biological replicates). (C) Annexin V/PI apoptosis assay following 48-hour exposure to TKI as single agents or in combination with WSD-0628 in FLT3-ITD resistant cell lines. Values presented as mean ± SEM (ordinary one-way ANOVA; n=3 independent replicates). (D) Phosphorylation changes in proteins regulating the activation of DNA damage and repair following treatment with ATM inhibitor alone, and in combination with sorafenib, or quizartinib, measured by Western blotting. (E-J) MV4-11 FLT3-ITD resistant cell lines were injected into the lateral tail vein of NOD-Rag1null IL2rgnull (NRG) mice. Treatment commenced once BLI reached a mean radiance of 1×10^6 p/s. Sorafenib, quizartinib, and WSD-0628 were administered once daily for 4 weeks. (E-F) *In vivo* monitoring of leukemia burden using bioluminescence BLI imaging over time (representative BLI images presented, shaded area indicates treatment time) of mice treated with WSD-0628, sorafenib or the combination. (G) Kaplan-Meier survival analysis of MV4-11–Luc+ FLT3-ITD resistant cells (n= 8 mice per group, shading indicating treatment duration) treated with WSD-0628, sorafenib, or combination (Log-rank, Mantel-Cox). (H-I) Monitoring of leukemia burden in the second study using bioluminescence BLI imaging over time (representative BLI images presented, shaded area indicates treatment

903 time) of mice treated with WSD-0628, quizartinib or the combination. (J) Kaplan-Meier survival
904 analysis of MV4-11–Luc+ FLT3-ITD resistant cells (n= 8 mice per group, shading indicating
905 treatment duration) treated with WSD-0628, quizartinib, or combination (Log-rank, Mantel-
906 Cox). Significance threshold of *p<0.05, **p<0.01 and ***p<0.001.

907

908 **FIGURES**

Figure 1

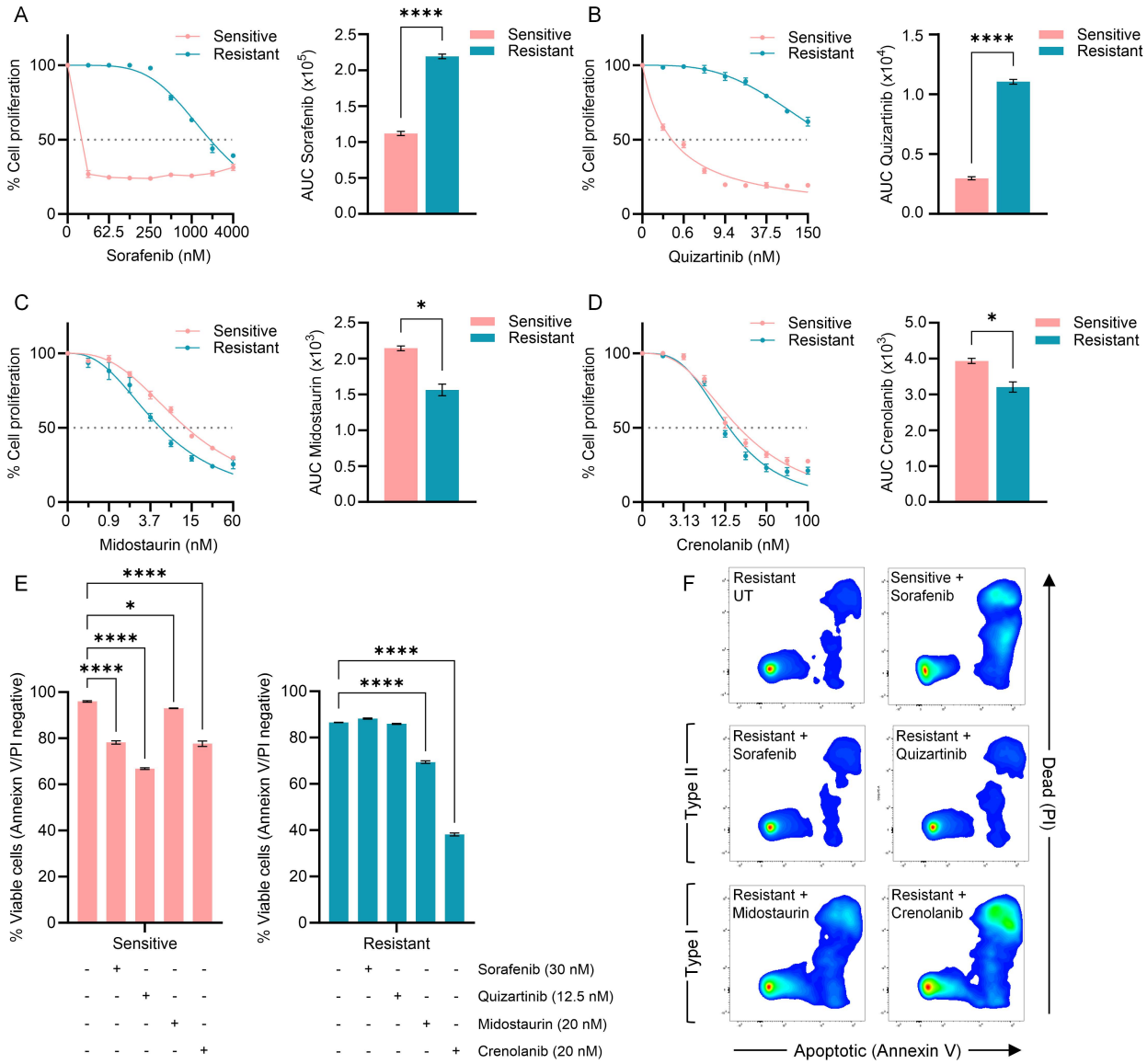

Figure 2

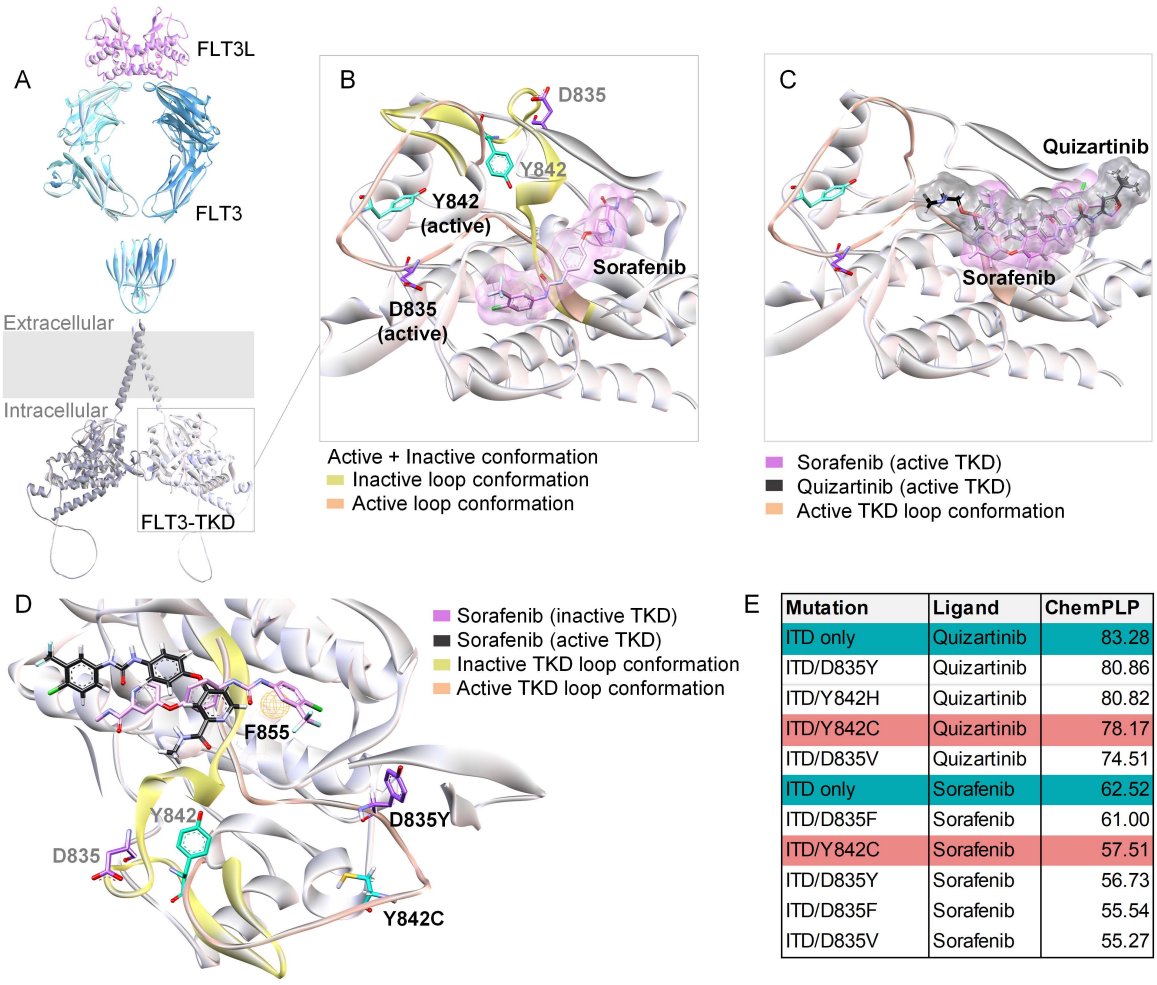

E

Mutation	Ligand	ChemPLP
ITD only	Quizartinib	83.28
ITD/D835Y	Quizartinib	80.86
ITD/Y842H	Quizartinib	80.82
ITD/Y842C	Quizartinib	78.17
ITD/D835V	Quizartinib	74.51
ITD only	Sorafenib	62.52
ITD/D835F	Sorafenib	61.00
ITD/Y842C	Sorafenib	57.51
ITD/D835Y	Sorafenib	56.73
ITD/D835F	Sorafenib	55.54
ITD/D835V	Sorafenib	55.27

Figure 3

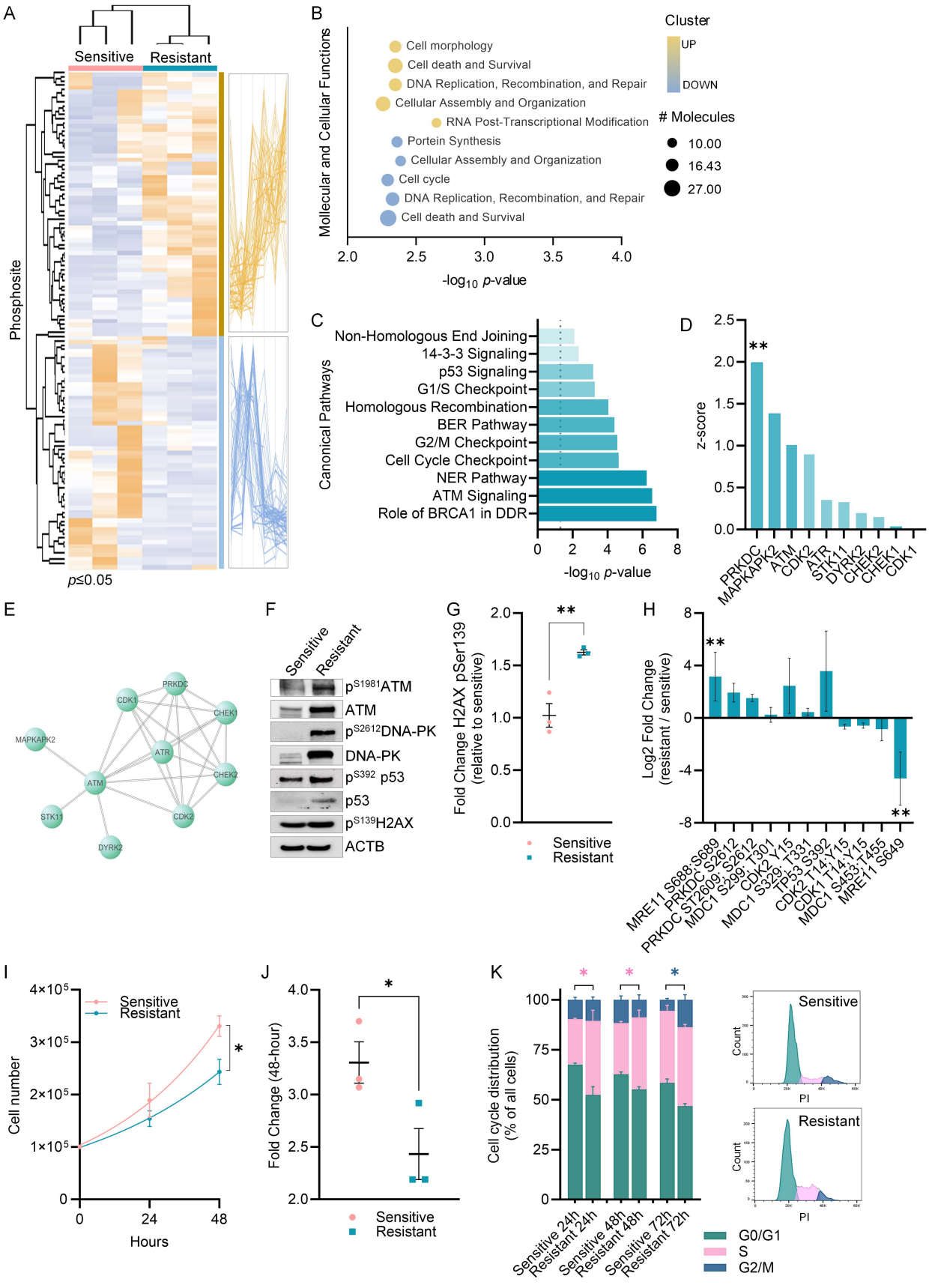

Figure 4

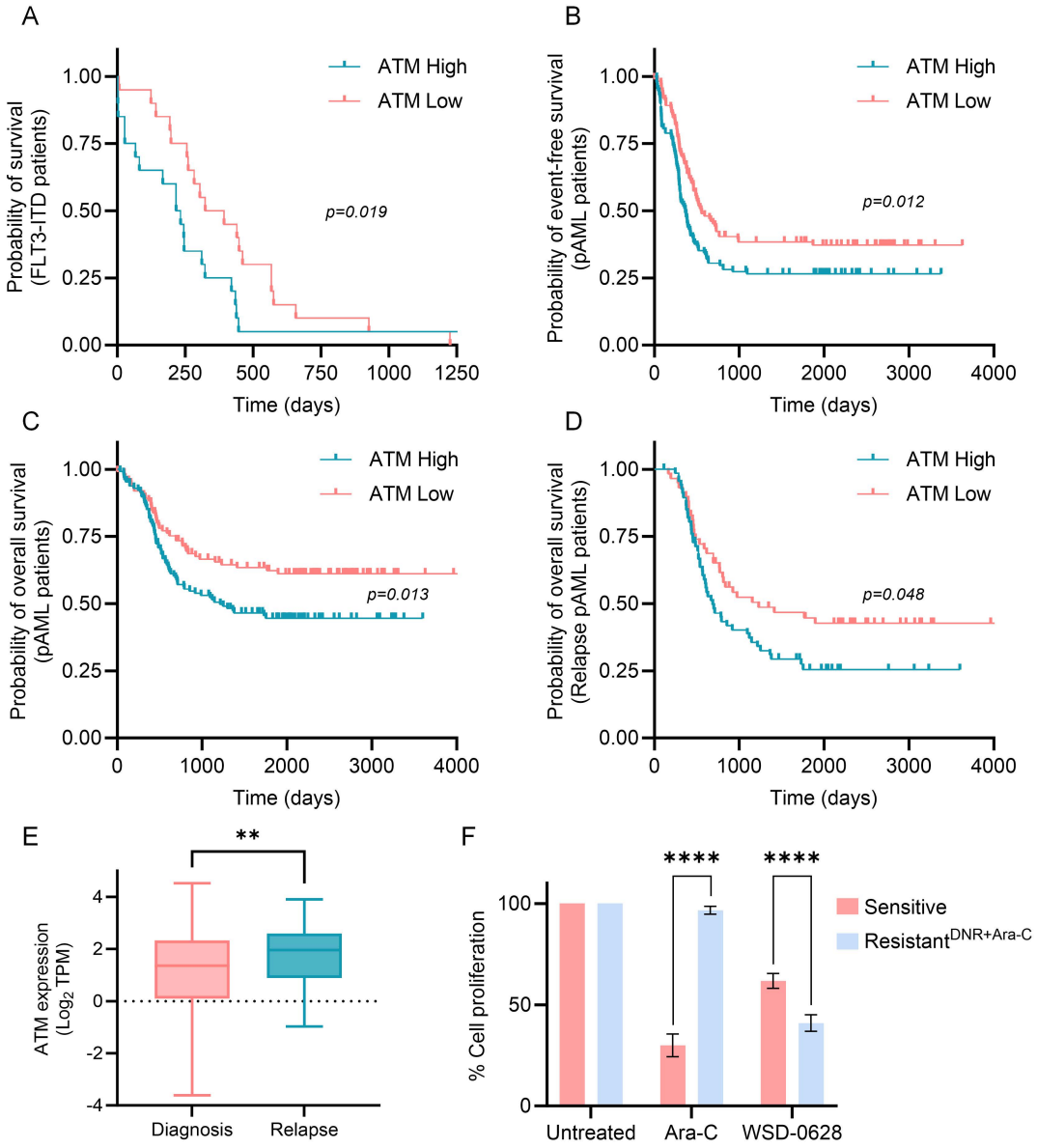

Figure 5

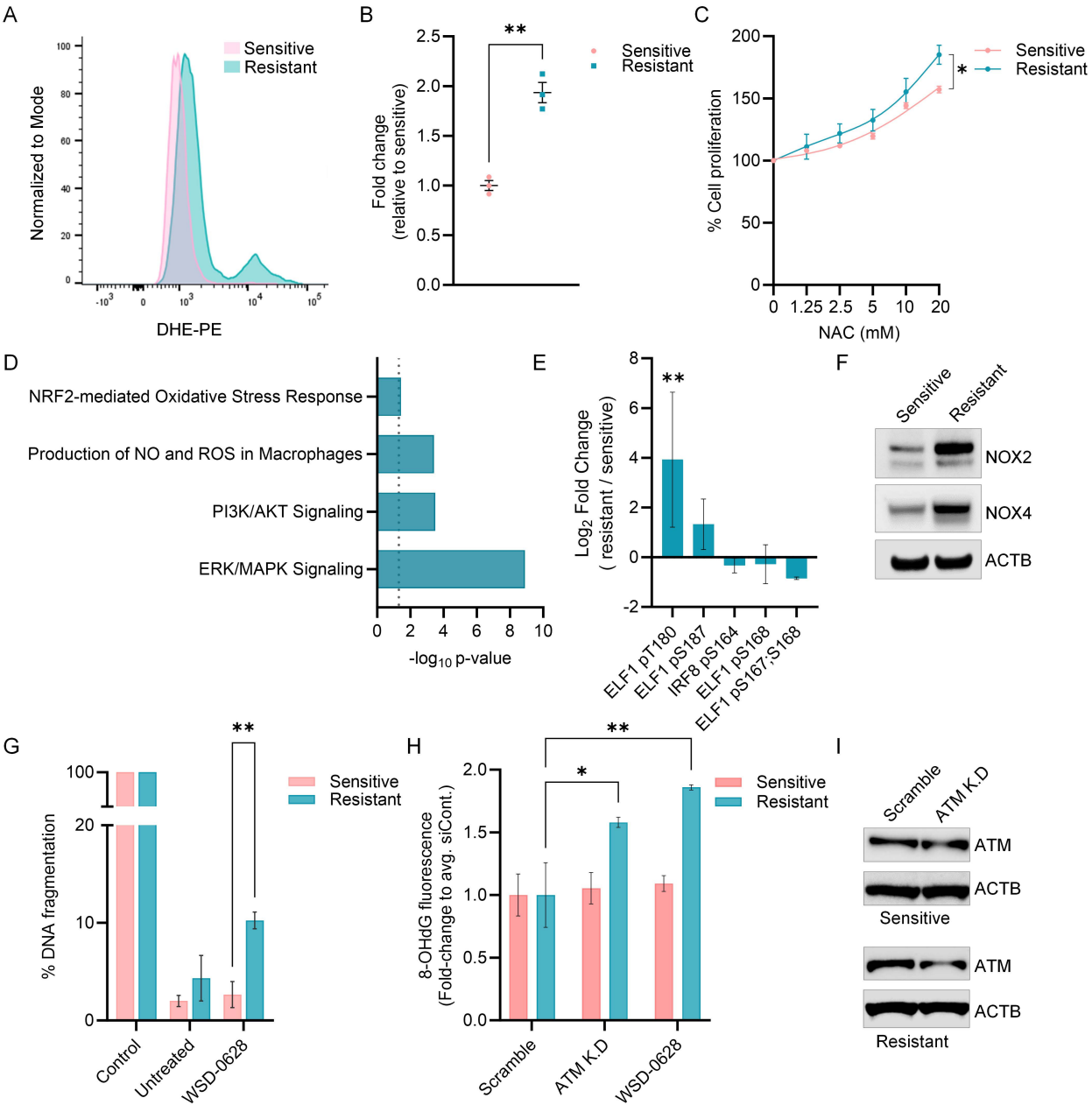

Figure 6